

Quarterly Summary

October - December 2017



MMT Staff from left: M. Abd Rahim, J.T. Williams, W. Goble, M. Guengerich, J. DiMiceli, E. Martin, R. Ortiz, S. Kattner, B. Russ, M. Anaya, D. Gibson, M. Alegria, J. Hinz, C. Ly, B. Weiner, K. Duffek, B. Comisso, G. Williams, C. Knop, T. Oldham, M. Lacasse, J. Wood, D. Porter.

Not Pictured: C. Chang, B. Kunk, A. Milone, T. Pickering, K. Powell, T. Trebisky, S. Schaller; *Students:* B. Lara, C. Oswald, A. Williams

MMT Observatory Activities

Our Quarterly Summary Reports are organized using the same work breakdown structure (WBS) as used in the annual Program Plan. This WBS includes a major category with several subcategories listed under it. In general, many specific activities might fall a tier or two below that. The WBS will be modified as needed in future reports.

Administrative

Program Management

The annual staff meeting and photo took place at the summit on October 31. Lunch was provided, followed by the “State of the MMTO” address by Director G. Williams, and then the staff photo.

Staffing

During this quarter, K. Duffek has continued consulting with the TAO (Tokyo Atacama Observatory) group at the request of group leader Tom Connors of Steward Observatory. TAO has been getting closer to testing their 6.5-m mirror support system using a dummy mirror. K. Duffek has provided input on systems checkout, failure mode resolution, and overall expected system performance.

K. Duffek has also consulted with the Vatican Observatory this quarter, where he was previously their Operations Manager. He has participated in meetings to help his replacement learn the new Vatican Telescope mount control system originally designed by K. Duffek, as well as to impart knowledge on other Vatican Telescope legacy systems.

Reports and Publications

There were 25 peer-reviewed publications during this reporting period. See the listing of publications in Appendix I, p. 28.

Presentations and Conferences

M. Alegria attended the Site Managers Conference in Denton, TX on October 10 and 11. The conference was hosted by the University of North Texas, Denton. The attendees included representatives from Apache Point, Las Campanas, Lick, Lowell/Discovery, Magdalena Ridge, McDonald, Monterey Institute for Research in Astronomy, Tarleton State University, and Winer observatories/telescopes.

Topics of discussion included:

- Mirror cleaning methods and practices - routines, methods, time scales, issues
- Mirror coatings - types, measurements, performance
- Dark skies - monitoring, preservation, public outreach
- Personnel - hiring, training, safety practices

MMTO methods and data were shared with the group. They were used quite extensively in the group discussions. General consensus was that we are a very high-performing staff, and we continue to help further observatory best practices and scientific returns in the astronomical community.

P. Schaller and T. E. Pickering attended the 27th annual Astronomical Data Analysis Software and Systems (ADASS) conference held October 22-26 in Santiago, Chile. This year's meeting had a much larger emphasis on operations and data pipeline software than previous meetings. T. E. Pickering also attended the following tutorials at ADASS:

- Using Docker “containerization” to simplify deployment and management of observatory computing systems.
- Asynchronous programming in Python.

T. E. Pickering was invited and attended the 9th annual Astronomy Conference hosted by SAAO, held November 14-17 in Cape Town, South Africa.

Safety

Nothing to report

Primary Mirror

On November 29, the primary mirror was prepared for washing. On November 30, a wet wash was done using 3% Liqui-Nox (soap) and water.

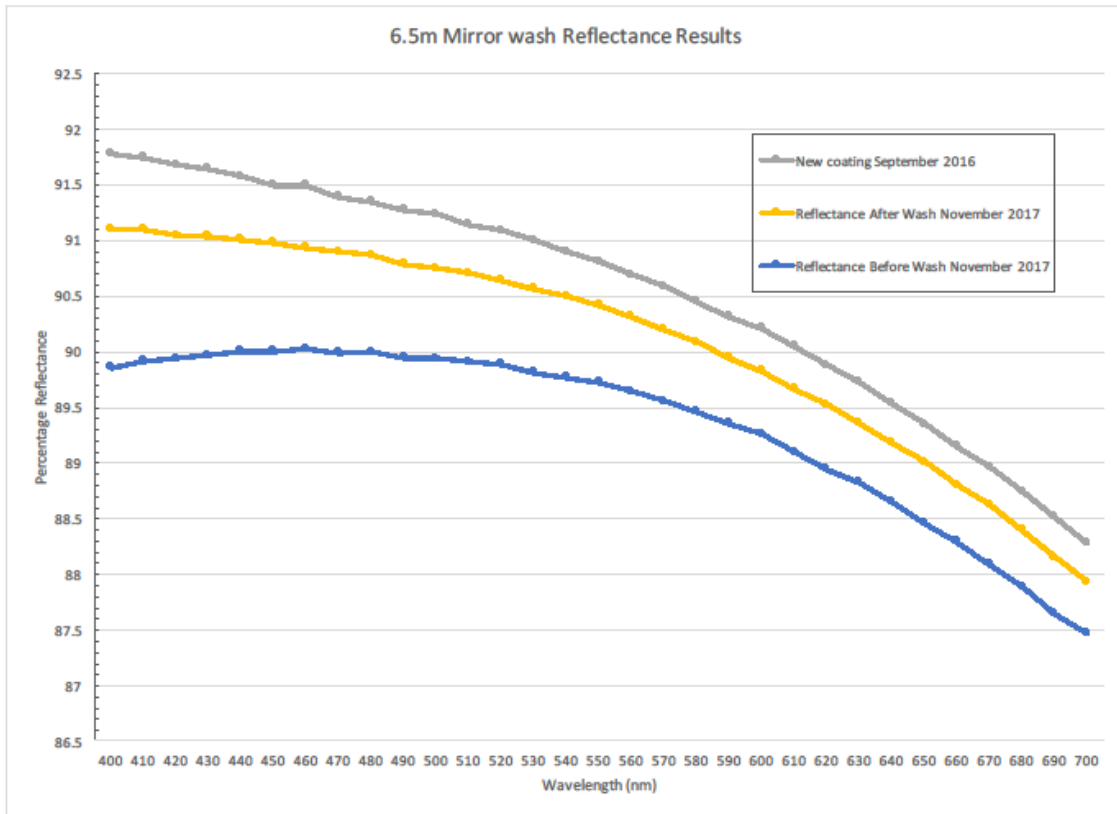


Figure 1. Measurements of the reflectance of the primary mirror before (blue) and after (yellow) the November 2017 contact wash. Also plotted (gray) is the reflectance of the primary mirror after recoating in September 2016.

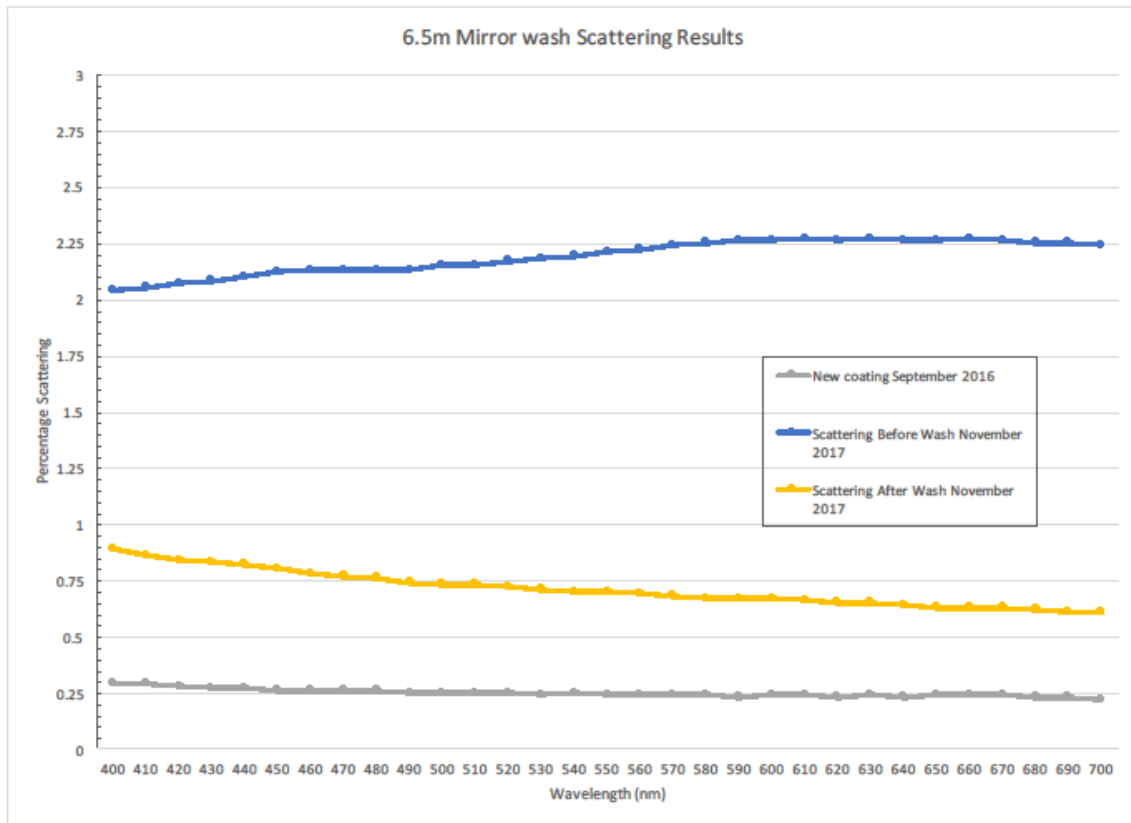


Figure 2. Measurements from the scattering from the primary mirror before (blue) and after (yellow) the November 2017 mirror wash. Also plotted (gray) is the scattering measurements following the recoating in September 2016.

Data Analysis

A series of Python Jupyter notebooks were created by B. Lara (recent undergraduate student hire and computer science/physics major). These notebooks investigated data quality and noise levels for primary mirror (M1) actuators and hardpoints, dewpoint and relative humidity sensors, and M1 glass temperatures.

M1 cell actuator data from the past year was evaluated for standard deviation and other statistical parameters under four different operational conditions: 1) blue-red spectrograph mounted with the M1 ventilation system off, 2) blue-red spectrograph mounted with the M1 ventilation system on, 3) blue-red spectrograph mounted with the telescope at zenith, the M1 mirror at the “magic” position, and the M1 ventilation system off, and 4) blue-red spectrograph mounted with the telescope at zenith,

the M1 mirror at the “magic” position, and the M1 ventilation system off. Data with the blue-red channel spectrograph installed were chosen because these data are believed to have the least amount of electrical, mechanical, and thermal noise data compared to other instruments. Noise levels are also thought to be lower with the ventilation system off. The “magic” position for the primary mirror is where it is fully raised in its normal operational position. The difference of the actuator-commanded force minus the actuator-measured monitor values was examined for both single and dual actuators from 2016-10-31 to 2017-10-31. This difference parameter was investigated to determine relative noise levels.

A variety of features were found in the data. Perhaps most significant is the dependency of the noise level on different electrical power supplies. Varying noise levels were found in the data corresponding to different power supplies. After the data analysis, the power supply with the lowest M1 cell actuator noise was re-installed on the telescope. Similarly, the M1 cell hardpoint data from 2017 were analyzed for the same four scenarios as the M1 cell actuators. Regardless of the scenario, standard deviation of hardpoint data was found to be high during November and relatively low during other months during 2017. The variations in hardpoint noise are still being investigated. Both the M1 cell actuator and hardpoint Jupyter notebooks will be used for further data analysis.

Chamber and outside dew point and relative humidity data were also examined for data quality. Four sensors currently measure relative humidity and dewpoint, either directly or indirectly: Vaisala2, Vaisala3, Vaisala4, and Yankee. Of these, only the Yankee thermohygrometer directly measures dew point with a chilled mirror. The Vaisala sensors measure relative humidity with a dew point calculated from these values. Of these Vaisala devices, only the Vaisala2 has a heated relative humidity sensor. This heated sensor allows the sensor to dry out more quickly after moisture saturation. The Yankee and Vaisala2 sensors are located in the telescope chamber while the Vaisala3 and Vaisala4 are located outside.

Figure 3 presents a sample of the dew point and relative humidity data. Data from the Yankee and Vaisala2 devices were sampled for the past year (2016-09-01 to 2017-10-01) under conditions where the front shutters were closed. In the range of 5% to 95% relative humidity, the calculated dew point from the Vaisala2 was found to be within 0.5°C of the measured Yankee dewpoint. This suggests good correlation between the two sensors. The calculated Vaisala2 dew points are erroneously very negative at very low (<5%) relative humidity. Very few sample points are found above 95% since data were restricted to conditions where the chamber was closed. A detailed report is planned for these weather and environmental data analyses as the weather initiative continues into the next fiscal year.

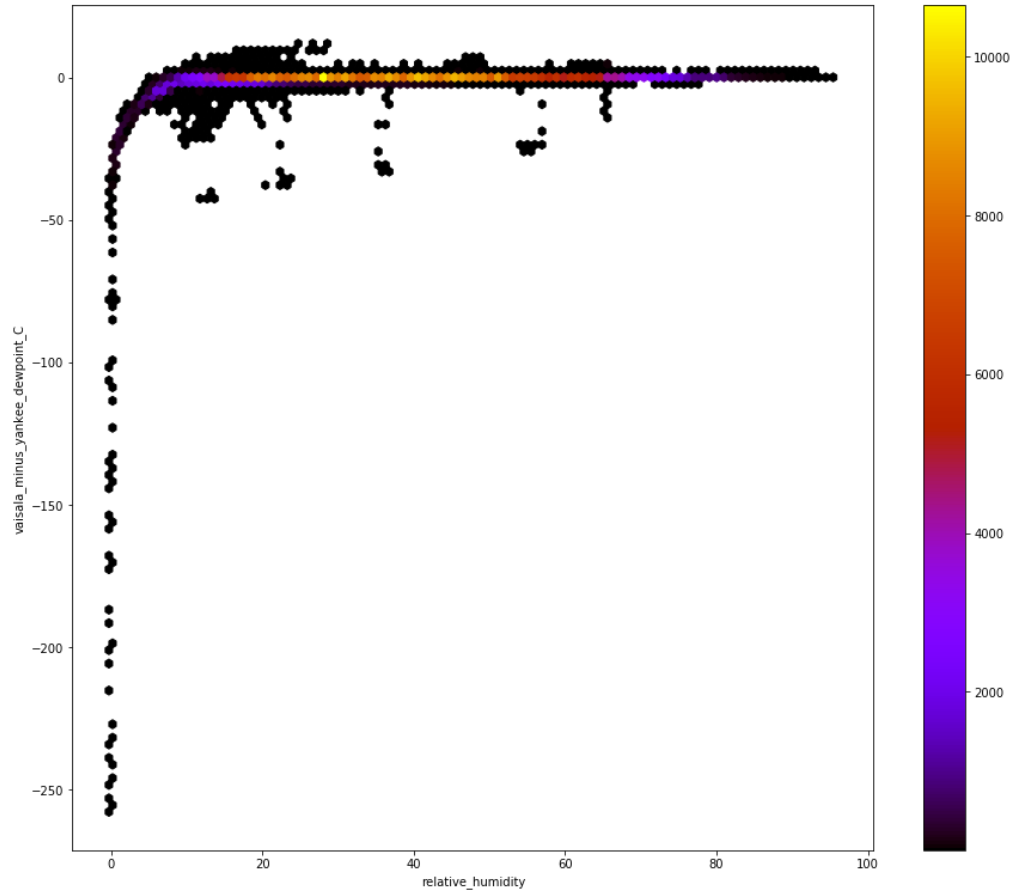


Figure 3. A “hexbin” map plot of relative humidity (in %) on the x-axis versus the difference (in °C) in the Vaisala2 calculated dew point minus the Yankee dew point on the y-axis. The concentration (*i.e.*, number of data points) in each hexbin is shown in the color legend at the right of the figure. Data are from 2016-09-01 to 2017-10-01. Data are restricted to conditions when the telescope chamber is closed. See text for more details.

Actuators

Actuator 143 was taken out of service because it was reporting panics. With cell air off, it had a +75 to 80lb monitor force. It was replaced with a known working actuator but the replacement actuator failed to work when a bump test was performed. While troubleshooting the replacement actuator, we found the +48V supply was not present on the servo board. It was determined that the +48V fuse on the power distribution board had been blown. A replacement fuse was installed and a bump test was performed and it passed with no issues.

The actuator test stand was employed to test the single axis actuator 143 that was removed from location #143 in the cell. After hooking up the actuator for a test, it was found that the test stand had a blown 48V power supply fuse. An initial inspection found loose hardware in the power supply unit. It was removed, and the fuse was replaced. Initial testing was nominal (no actuator connected). A discussion about why the fuse blew led us to the actuator under test with a faulty 48V DC/DC

converter. The DC/DC converter was replaced, and the actuator was tested on the test stand with no failures.

A 3D model of a single-axis actuator was created by A. Williams at the request of W. Goble. A. Williams reorganized an already existing excel sheet containing archived engineering drawings, and after which I created a new spreadsheet containing pre-existing Autocad drawings was created. Using both spreadsheets A. Williams was able to locate drawings of various parts and assemblies needed to recreate the actuator using SolidWorks 2016 software.

Secondary Mirrors

f/9

During an f/9 run on December 22, barbell star images were seen on the SOGUIDER. After troubleshooting, it was determined that the f/9 SE axial hardpoint was oscillating. Power cycling the mirror support and changing telescope elevations had no impact on the image oscillations. At the time the temperature was very cold (15-20° F). As the temperature warmed up, the amplitude of the oscillation reduced. By the time a repair crew arrived at the telescope, the temperature was warmer, and the malfunction could not be duplicated. The most likely cause is the SE axial air transducer or the SE axial electronics card. A spare transducer was modified, per schematic, with a resistor in line with the input voltage, inside the DB9 connector backshell. The SE axial air transducer will be replaced, if needed.

Hexapods

f/9 and f/15 hexapod

The three UMAC cards sent to Delta Tau for repair were returned. The CPU module and fiber module both required repair while the power supply had no defects. Testing of the spare units hasn't been done yet.

On November 7, the telescope operator reported several hexapod pods (A, B, E, and F) at positive and negative limits. Initially, restarting the Turbo UMAC corrected the malfunction. On November 14, the suspect ACC24E2A (Unit 1) from the Turbo UMAC rack was replaced with the spare module. Resistor SIPs, pull ups for limit switches, were swapped from the old module to the spare module. Address switches and jumpers were verified. The spare module was installed and the hexapod was tested. Each pod was moved individually and then platform moves were completed successfully. The faulty module was sent to Delta Tau for repair.

Optics Support Structure

Nothing to report.

Pointing and Tracking

Nothing to report.

Science Instruments

f/9 Instrumentation

The f/9 instruments were on the telescope for about 50% of the available nights from October 1 – December 31. Approximately 54% of those nights were scheduled with the Blue Channel Spectrograph, 35% with Red Channel, and 11% with SPOL. A total of 534.3 hours were allocated for f/9 observations. 26% of these hours were lost due to poor weather. 1.5% of time was lost due to instrument, facility or telescope problems, such as M1 panics or secondary oscillation issues. Blue lost 22% of its time to bad weather, with Red Channel losing 29%, and SPOL losing 40%.

f/5 Instrumentation

MMIRS was on the telescope October 12-20 and October 27-November 6. Observations were run almost all in queue mode, with classical observations requested by J. Yang for October 27-30. The classical observations were supervised by queue observer C. Ly.

The October 12-20 run was an unexpected one, one that was organized after the Hecto fiber-positioner failure. To fill the schedule quickly, all programs that had not been completed in the August 31-September 8 MMIRS run were added to the queue. In addition, three programs that had submitted targets in advance of the October 27-November 6 run (Kenyon, Ly, Willmer) were also added to the queue. In this run, 17.95 hours (20.6%) were lost to poor weather.

The October 30-November 6 run was intended to be one queue combined with the planned November 29-December 5 run. The mask design deadline was September 25, and four new masks were cut at SAO with the Binospec mask-cutter. This early November run sustained heavy weather losses. Some time was also lost due to the fact that the known 7-degree rotator instrument offset was not re-introduced after the instrument was powered down during bad weather. The late November run was lost completely due to the MMIRS vacuum leak. About 63 hours (69%) were lost to poor weather in the non-canceled time, while losses to the vacuum leak were 83.3 hours (51.6%) out of the originally scheduled runs.

Also canceled was the planned December 27-January 8 run, again due to the vacuum leak. Mask designs were due on November 23, and fourteen masks had already been cut with the Binospec mask-cutter at SAO for this run by the time of cancellation.

Despite the losses, MMIRS completed six programs in full, partially completed four programs, and made progress for an ongoing ToO program. This left three programs with no data at the end of 2017.

B. Weiner participated in Binospec commissioning runs in November and December, and he continues to communicate between MMTO and SAO staff on observing planning, data handling, and other issues. The MMT queue observing interface has been updated to handle Binospec programs, track masks, and to display the installed and pending Binospec masks. These interface updates were made by D. Porter.

f/15 Instrumentation

MAPS development from October through December was focused almost entirely on actuator electronics board development. The single actuator test fixture (SAT) was used to test our various electronics board configurations, and to troubleshoot electronics and firmware issues. These issues have put the project behind schedule. However, a stable board configuration was achieved near the end of December. In addition, the actuator body, bobbin, coil, and magnet have now all reached prototyping configurations.

The next step will be to use the nineteen-actuator test fixture (NAT) to develop the actuator controller and to test the configuration optically. To this end, the nonlinear simulation has been developed and will be calibrated using test data. The simulation can then be used for rapid prototyping of the voice coil controller, and it will be verified using an optical interferometric test stand being set up in the MAPS laboratory.

Topboxes and Wavefront Sensors (WFS)

Wavefront Sensor Software

All wavefront sensor (WFS) systems are now using the updated software for wavefront analysis. Work has been ongoing to improve the new analysis software to optimize performance and robustness. Support for the Binospec WFS was fully implemented and demonstrated. Some improvements have been made to the web interface, including support for continuous wavefront sensing.

Binospec WFS

Binospec has its own built-in WFS that patrols an off-axis region of sky to allow for continuous operation during science observations. The hardware is very similar to the WFSs on MMIRS, though Binospec only has a single unit. Early in the November commissioning run it became clear that the aberrations measured by Binospec's WFS were quite wrong. One didn't even need analysis software

to see this. The WFS images were aberrated in ways that on-axis images taken with the single-object guider were obviously not.

During the course of the two commissioning runs, a large amount of data was taken with the Binospec WFS to try to characterize the problem. The current theory is that the WFS's pick-off mirror is attached at the wrong angle. This then causes the light to enter the WFS at an angle which leads to aberrations due to the internal optics, as well as some magnification of the off-axis aberrations inherent to the MMT's optics.

As a workaround to at least enable periodic wavefront sensing, we developed a scheme that uses the single-object guide camera to perform on-axis curvature wavefront sensing (CWFS). This scheme involves taking a pair of images with the telescope focus changed by the same amount inside and outside of focus. We use +/- 1000 um of M2 focus change, which provides a good balance of signal-to-noise, pupil sampling, and calculation time for our needs. The pair of images is then analyzed using the LSST's CWFS analysis software (<https://github.com/bxin/cwfs>). The only modification that was required to make this software work for the MMT was to add a configuration file containing the MMT's optical specifications.

Once demonstrated to work, the LSST CWFS outputs were integrated with the new MMT WFS software to calculate and apply corrections. A web interface was developed to simplify carrying out CWFS analysis (Figure 4).

Binospec Curvature Wavefront Sensing

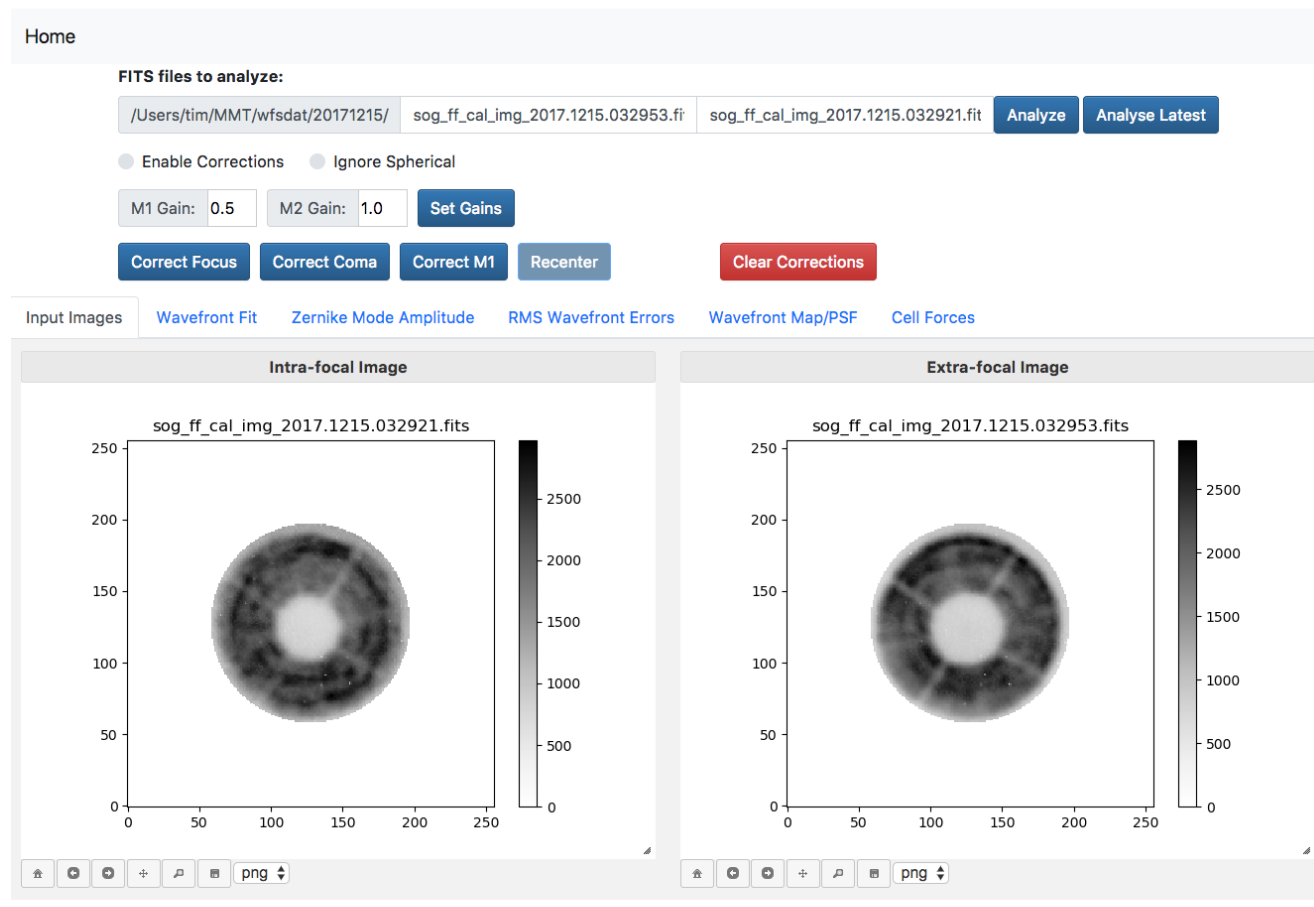


Figure 4. Screenshot of web interface for Binospec CWFS.

MMIRS WFS

The patrol regions for the MMIRS guide/WFS cameras are complicated “banana-like” shapes that bracket the field of view of the instrument. Due to the narrowness of some parts of these regions, it is not uncommon for parts of a WFS spot pattern to be missing because part of the star’s pupil falls outside the patrol region. Because the pickoff mirrors that define the patrol regions are angled, the

size of the pupil on the mirror is a function of position of the star. The WFS analysis software can handle missing sections of the pupil up to a point, but becomes more unreliable if a significant portion is missing.

B. McLeod worked out a way to predict pupil vignetting of MMIRS guide stars as a function of field position. Figure 5 shows some examples of predicted guide star pupil images. The areas in green are reflected into the guide/WFS camera, while the areas in red are not, and would yield missing WFS spots. Figure 6 shows how the predicted missing spots match up with actual WFS data. They match very well! Work is ongoing to implement these predictions into the WFS analysis software.

Another issue we discovered with MMIRS WFS data is that there are systematic outward spot displacements in apertures near the outer edges of the pickoff mirrors. This is likely due to the outer edges of those mirrors being slightly turned down. In addition to predicting missing spots, the analysis code will also need to flag and mask out apertures that are affected by the turned edges in order to avoid systematic errors in the wavefront measurements.

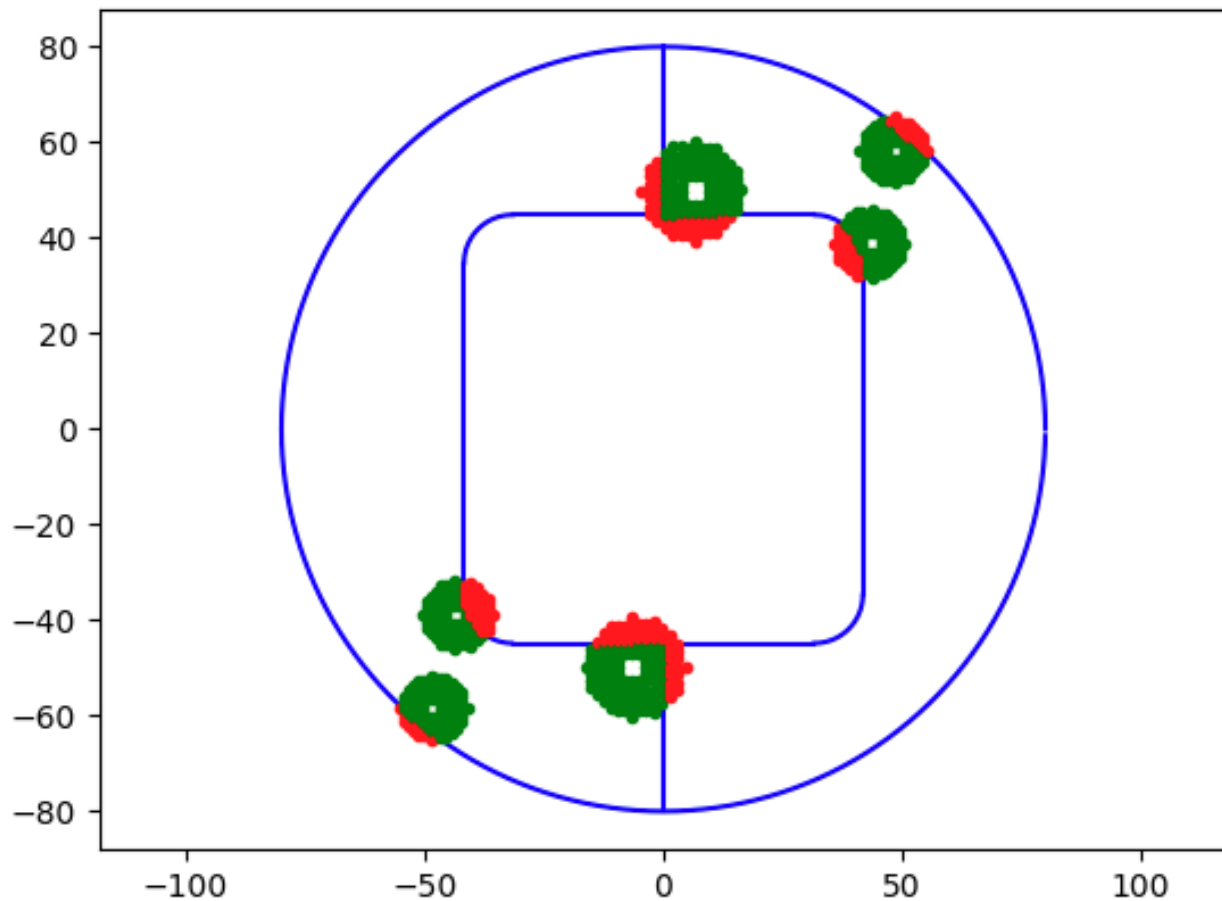


Figure 5. Pupil images of MMIRS guide stars at different field positions.

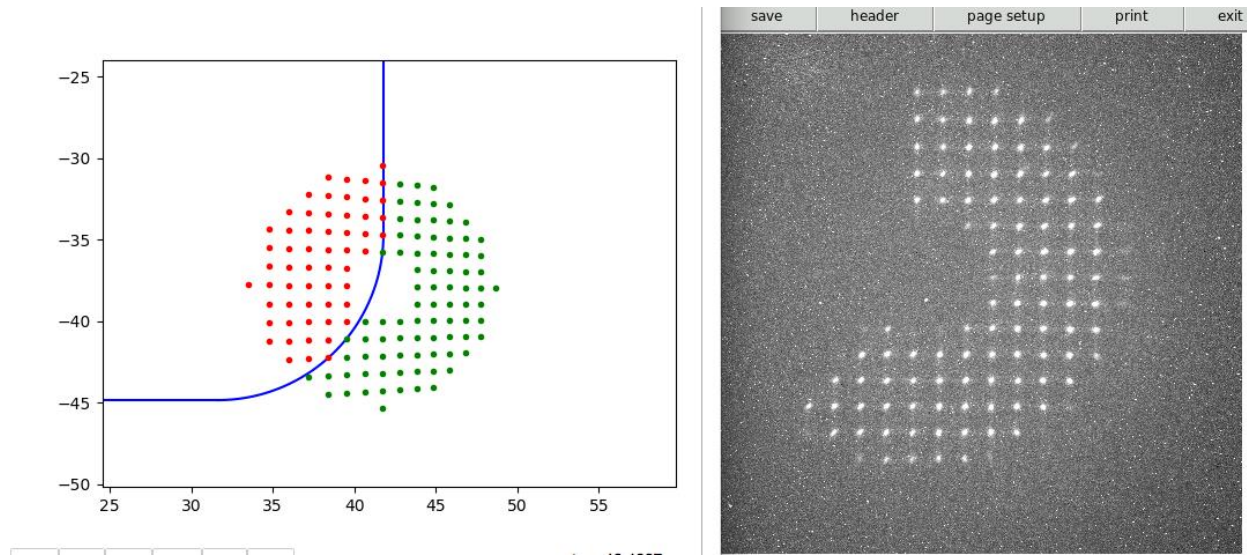


Figure 6. Predicted missing spots along with actual MMIRS WFS data taken at the same position.

f/9 Topbox

It was verified that the intensity control on the f/9 videoscope had no impact on the image. The 26-pin high density (HD) connector on the topbox was inspected, and a broken wire was found on pin 20. A short jumper cable with a 26-pin HD connector and a CPC was installed. A CPC connector was installed on the cable from the drive arc. The videoscope was connected to the drive arc, and it tested good.

A new web-based interface to the f/9 WFS camera was developed and deployed. It is based on the design of the MATcam interface, and it uses the same JS9 widget for image display and manipulation. A screenshot is shown in Figure 7.

F/9 Wavefront Sensor Camera Interface

Engineering Interface

Enable Cooling Set Temp (°C):

Camera Temp: -25.1 °C **Cooling Power:** 29.4%

Exposure Type: Exposure Time (sec):

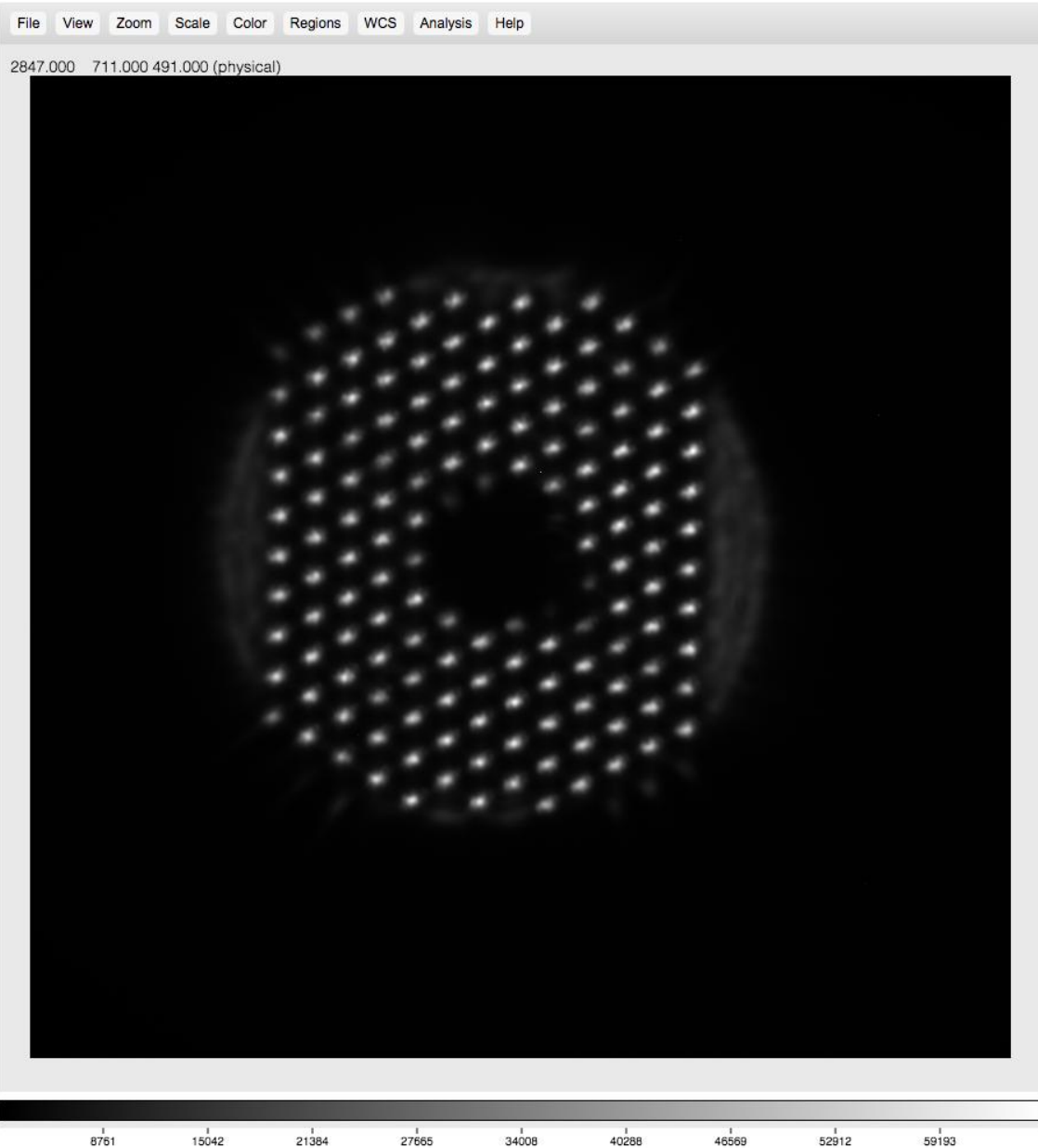


Figure 7. Web interface for f/9 WFS camera.

Facilities

Main Enclosure

The building drive has continued to function quite well since the LVDT (Linear Variable Differential Transformer) mount has been serviced. The electronics group has been troubleshooting the rotation-dependent problem of servo Card A building drive spare. So far, the problem has been traced to the LVDT section of the board. The problem seems to be an apparent warm-up issue suspected to be a capacitor or voltage regulator. An M&E night in January has been selected for further troubleshooting.

The new Carrier3 BACNET fiber connection was installed in November. A router and fiber converter were installed inside the chiller unit, a fiber converter was installed in the MGE room carrier enclosure, and conduit was run from the chiller to the MGE room Carrier enclosure. A multimode fiber was run between the fiber converters via the conduit, enabling network connection. The system was tested and, with minor changes, we were able to communicate with Carrier3 over the network. Carrier2, Carrier3, and VFD blower systems were documented in ORCAD, and printed in PDF format.

Instrument Repair Facility (IRF)

The clean room in the IRF became fully operational the last week of November.

General Infrastructure

During the week of October 9, the annual inspection and maintenance of the microwave link between the MMTO and Steward Observatory on campus was performed by Logicalis.

Computers and Information Technology

Monthly backups of *mmto* and *hacksaw* were done, along with reboots to pick up new kernels and virtualbox drivers. Pending updates were installed on *nas1*, *nas2*, and *nas3*. *Hacksaw* was upgraded to Fedora 26. Minor problems with the rsyslog daemon, the lightdm login screen, the sendmail daemon, and the LDAP server were addressed.

Modifications were made to the `hexapod_linux` code, improving the code with respect to timeouts, i.e. so that the code doesn't hang up when encountering new failure modes of the UMAC. Work will continue in this area.

An enhancement to the annunciator parameter editor was made to allow pull down menus for some parameters. A new annunciator check was implemented for the instrument rotator offset. Binospec was added to the settings server database.

Hardware/Software Interfaces

The queue scheduling software for MMIRS, described in previous quarterly reports, was modified to include the additional requirements of Binospec. The overall approach to queue scheduling remains the same for both instruments. However, upgrades in the underlying astropy, astroplan, and numpy Python libraries, and the additional requirements for Binospec, have resulted in significant changes to the scheduling code. These Python library upgrades include Python 2.x to Python 3.x, astropy 1.x to 2.x, and astroplan 0.2 to 0.4. The new scheduling software was used for both the November and December Binospec runs. The latter run included 168 observing blocks over a 10-day run. Software modifications were made as issues arose during these runs.

Three new Binospec-related constraints were added to the queue scheduling software: MaskAngleConstraint, MaskNumberConstraint, and TransitConstraint. The MaskAngleConstraint limits the deviation of the current observing parallactic angle from the design position angle for the mask. As with other constraints, the maximum score for the constraint is 1.0. The minimum score for the MaskAngleConstraint currently does not go completely to zero when targets would be outside the allowed constraint limits. This allows observing blocks to still be scheduled under these conditions, but with a low overall constraint score. The MaskNumberConstraint limits the number of masks available at any time for the instrument. This limit is currently ten masks for Binospec. This mask constraint is less important for Binospec than MMIRS since Binospec masks can be changed on a daily basis or even potentially during the night. The new TransitConstraint determines if the celestial meridian will be crossed during an observing interval. At the moment, only the MaskAngleConstraint is actively being used in queue scheduling. The MaskNumberConstraint and TransitConstraint are readily available for use, if needed.

New Redis parameters were created to clearly separate Binospec and MMIRS scheduling. These Redis parameters include the commands to start either dispatcher or scheduler computations for both Binospec or MMIRS. Any of these commands can be run simultaneously on the computer *cruncher*. Similarly, the computation status and output Redis parameters are also distinct for each instrument and computation mode. These parameters are read by the Observatory Manager to update user interfaces in real time using Redis' publish-subscribe paradigm.

An SQLite database has been added to the scheduling software for application-specific storage of computed constraints and of details of scheduling runs. This database serves as a cache for astronomical constraint scores that have previously been computed. Programmatic constraints, such as TimeAllocationConstraint, are always recomputed since they are highly dependent on previous scheduling. If a cached value for a constraint under similar target-time criteria is not found, a new constraint score is calculated and cached for later use. This database also allows for detailed review of the scheduling process.

Observer/PI Catalog Interface

The catalog submission interface for the Observatory Manager has been updated to support Binospec queue observing. The new interface was used for the previous two runs and based on feedback from those two runs, it has been tweaked to make it more user-friendly. Finalized features that differ from the previous catalog submission interface (the MMIRS version) are:

- Simplified layout with collapsible sections to save space.
- Integrated MMTCATVIZ, a new catalog visualization widget that interactively shows target positions on the sky.
- A new “wizard” style interface for submitting new targets. Rather than overwhelming the user with a complex input form, the wizard asks a series of questions to make the input simpler.
- When data is taken for a specific catalog target, the data automatically becomes available inside of the catalog target table for the PI. A new folder icon appears for targets with data, and links allow for downloading all or part of the dataset.

Submitted Binospec Masks

To create a mask, you will first begin a [New Target](#). Next, choose "Mask -> Create Mask" option and you will be instructed how to create your mask. After the mask is submitted, you will need to finish creating the target for your catalog.

- MS0451
- MS0451-2
- MS0451-3

MMTCATVIZ

18:56:13 MST Tuesday, January 30th 2018 MST 01:56:13 UTC

XY: (1218, 237)
 RADEC: (11:11:17.678, -2:19:01.962)
 ALTAZ: (45.29, 228.29)

MS0451-2
 Alt: 47.886
 Az: 140.790
 RA: 4:54:10.277 Dec: -2:58:03.550
 Rot: —

SDSS
 Button
 Zoom
 Reset
 Time
 Current
 Obs. Run
 Interactive

20:00 00:00 04:00 08:00 12:00 16:00 20:00 00:00 04:00 08:00 12:00 16:00 20:00 00:00 04:00 08:00 12:00 16:00
 Mon 29 January Tue 30 January Wed 31 January Thu 1 February

Catalog Targets (3) Submission Deadline: Monday, Dec 04 17:00:00

Column Filters: Priority ID ObjectID Offsets Observation Type Details Exposure Total RA DEC Epoch Progress

Priority	ID	Data	ObjectID	Offsets	Observation Type	Details	Exposure Total (sec.)	RA	DEC	Epoch	Progress
1	1036		MS0451	0	mask	MS0451	1 x 3 x 1200sec = 3600sec	4:54:07.811	-3:02:58.380	J2000	<div style="width: 100%;"></div>
2	1037		MS0451-2	0	mask	MS0451-2	1 x 3 x 1200sec = 3600sec	4:54:10.277	-2:58:03.550	J2000	<div style="width: 100%;"></div>
3	1038		MS0451-3	0	mask	MS0451-3	1 x 3 x 1200sec = 3600sec	4:54:26.296	-3:00:23.290	J2000	<div style="width: 100%;"></div>

Summary: 3 hours (exposures) + 1.33 hours (est. overhead) = 4.33 total hours

Figure 8. Observer Catalog Submission Page.

Queue Observer Interface

The queue observer web interface has been updated to make it possible to observe both MMIRS and Binospec queue programs. Some of the major features that have been added to the new interface are:

- Next block selection. This feature allows the queue observer to tell Binospec what the next target will be prior to finishing the current target. This allows the instrument to preconfigure itself for the next catalog target.
- The “Dispatcher” table has been enhanced to show more information, and also allow some additional information to be toggled on-and-off.
- The “Programs” table tab shows each program, and allows for toggling on-and-off specific programs to make it simpler to look for specific program targets. This table also shows a summary of catalog targets and program progress.
- A new tab called “Targets” was added. It shows a table of all targets submitted for the queue. This table is sortable by “target name,” “program number,” RA, DEC, and “progress.”

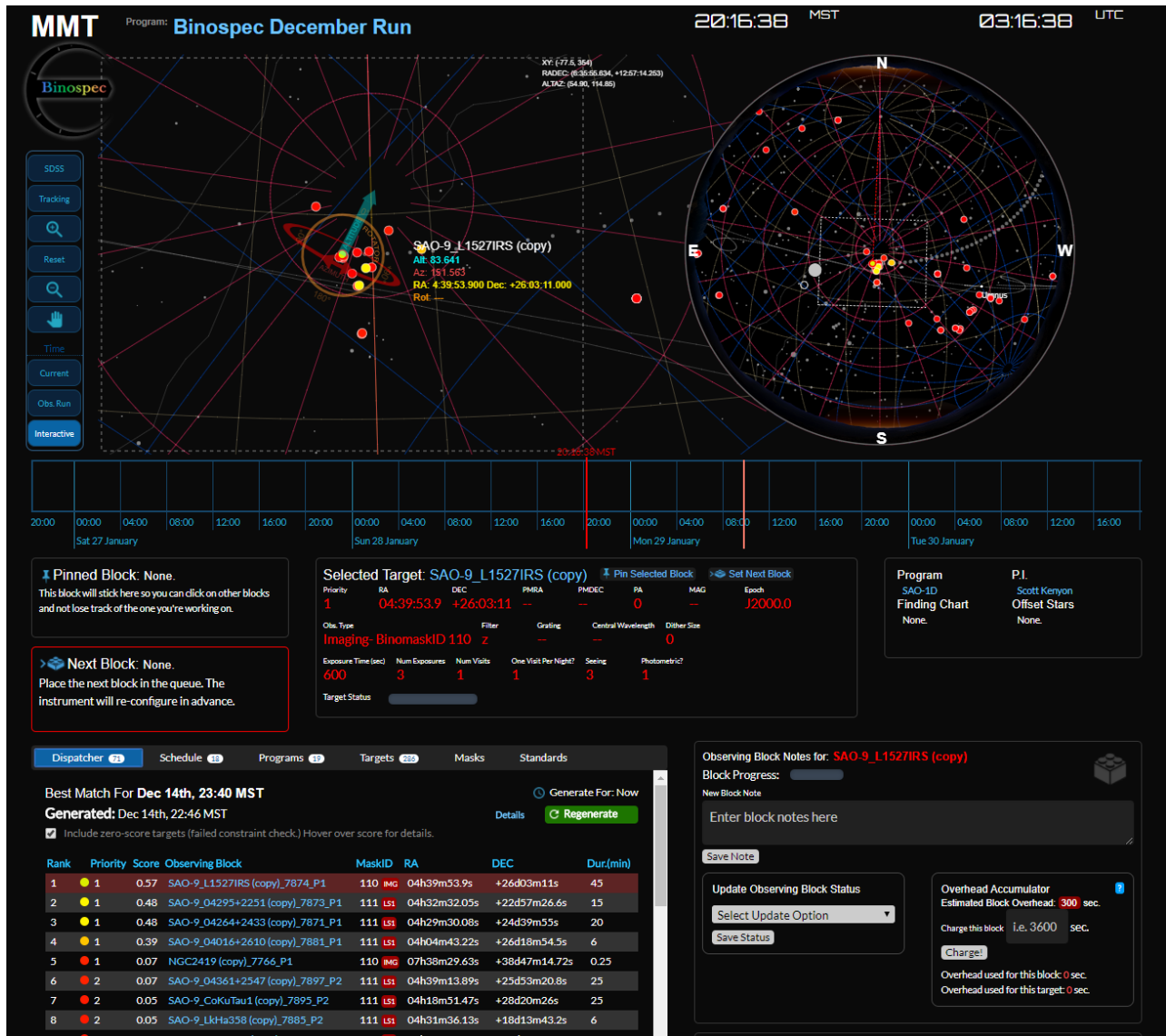


Figure 9. Queue Observer Web Interface.

MMTCATVIZ is a modular widget that is made from HTML and JavaScript, and can be plugged into any of the Observatory Manager pages. The interface shows two different sky projections: an RA/DEC projection that uses the X&Y axis (left side), and a polar projection that uses the MMT's zenith as the polar center. Below the two projections is an interactive timeline that automatically scrolls to the selected target's scheduled observing time. The timeline can be switched into "interactive" mode that allows the user to drag and zoom the timeline manually. As the timeline is changed, the two projections update automatically based on the selected date and time in the timeline.

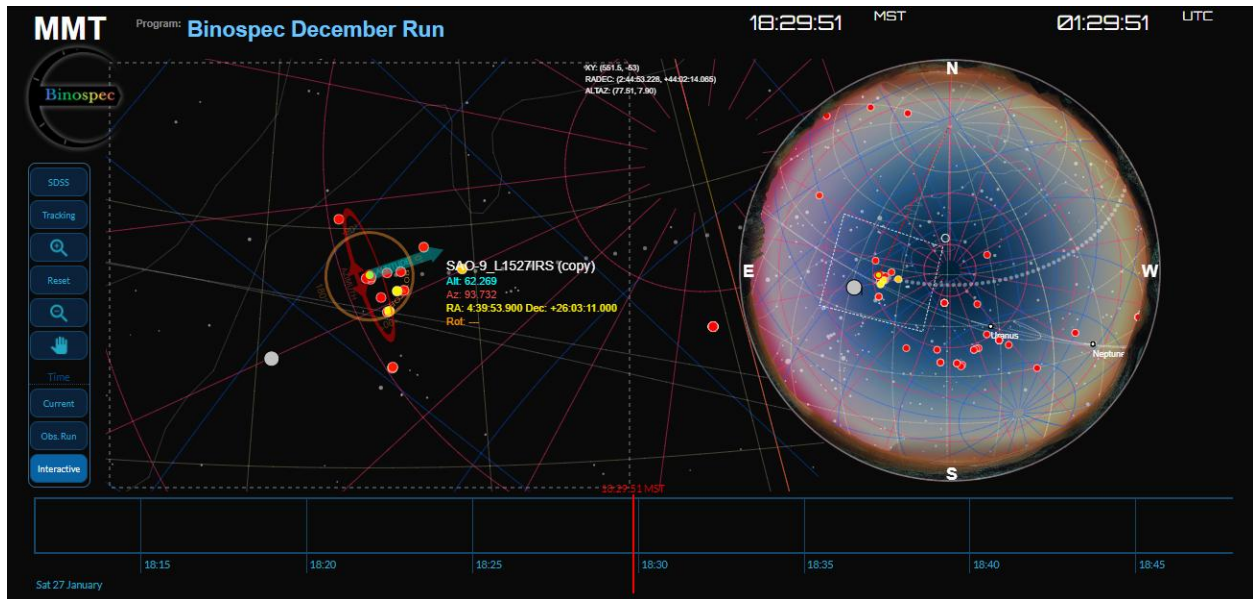


Figure 10. MMT CATVIZ Widget showing the transition from day into night.

Telemetry, Logging, and Database Management

A new logging approach is being evaluated using the ZeroMQ (<http://zeromq.org/>) distributed messaging library. This high-speed, highly versatile library can be used to transport data from a sensor attached to a small Raspberry Pi, for example, to one of our logging servers, such as *ops* or *ops2*. Support for the open-source ZeroMQ library is available in many languages and on many hardware platforms. The logging approach is distributed, allowing computers to act as servers and/or clients with communication between computers over the network. Clients generally sample data from hardware devices and then push that data to the servers, while servers receive data and log that data into files and databases.

A ZeroMQ server was written in Python, following the “Lazy Pirate” paradigm (<http://zguide.zeromq.org/py:lpserver>). This server logs data to comma-separated value (CSV) files and to a MySQL database on the localhost computer. Instances of the server are currently running on *ops*, *ops2*, and various Raspberry Pi’s. Multiple instances of the ZeroMQ server are running on different ports on these computers, allowing for immediate fall-over to a new port if a port is not available to clients.

ZeroMQ clients, also following the “Lazy Pirate” paradigm, have been written in PHP with additional similar clients planned in Python. These clients have extensive configuration parameters that determine where and how often data are sampled and logged. Clients have been written for a variety of data sampling protocols, including BACnet, RS232 serial port, and socket network protocols. Many of these protocols are unique to specific device manufacturers. Clients are currently running on *ops*, *ops2*, and various Raspberry Pi’s. Data are pushed to the MMT master *Redis* server, *dataserver2/annunciator*, and various MySQL databases so that the devices are integrated with existing telemetry and data presentation tools.

Weather and Environmental Monitoring

Weather Stations

An articulating boom was rented, and repair of RM Young was started. An initial inspection found several issues: the upper waterproof box had leaked, the electronic wiring terminal strip was immersed in water, and the multipair wire had water under the jacket. A new waterproof box was installed, and a new cable was run from the lower electronics enclosure to the “bird” junction box. Initial results showed improved data from the RM Young, but there are still occasional wind speed dropouts. It is suspected that the bearings may be bad on the propeller causing incorrect values at low wind speeds. Additional troubleshooting will be done when an articulating boom is rented again.

All Sky Camera and Web Cameras

The numerous hot pixels on the MMTO all-sky camera have long been a source of confusion for some users. T. Pickering used a set of images from a cloudy night to construct a bad pixel mask. An example of the results is shown in Figure 11. This bad pixel mask is now implemented in the pipeline for the all-sky camera and is applied to every image it acquires. It makes a significant improvement overall. There are still a few sporadic hot pixels that flash on and off at times, but they are mostly unobtrusive and easy to pick out in the all-sky animations. The mask is implemented as a FITS image, so updating the bad pixel mask only requires replacing that one file.

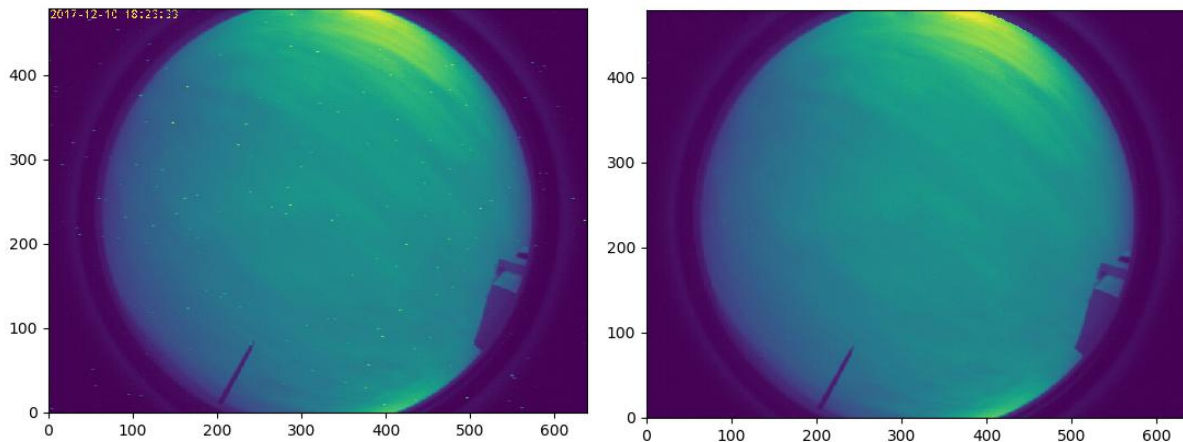


Figure 11. Sky camera images before and after applying bad pixel mask.

Seeing

The overall seeing histogram for the 4th quarter of 2017 is shown in Figure 12. There is a strong peak at 0.73”, but also a long tail, so the overall median seeing as-measured is 0.84”. The shape of the histogram is not as well-described by a log-normal distribution as it has been in previous quarters. There are two possible reasons why: 1) the new analysis software works much better in very bad seeing and thus can actually measure seeing values $>2.5''$. Therefore, it’s measuring more of the long tail of the spectrum of bad seeing; 2) the overall statistics are dominated by the number of measurements

taken during the Binospec (11099) and MMIRS (4136) runs. The November Binospec run had generally pretty good to great seeing, while the December run was characterized by poor weather and strong easterly winds.

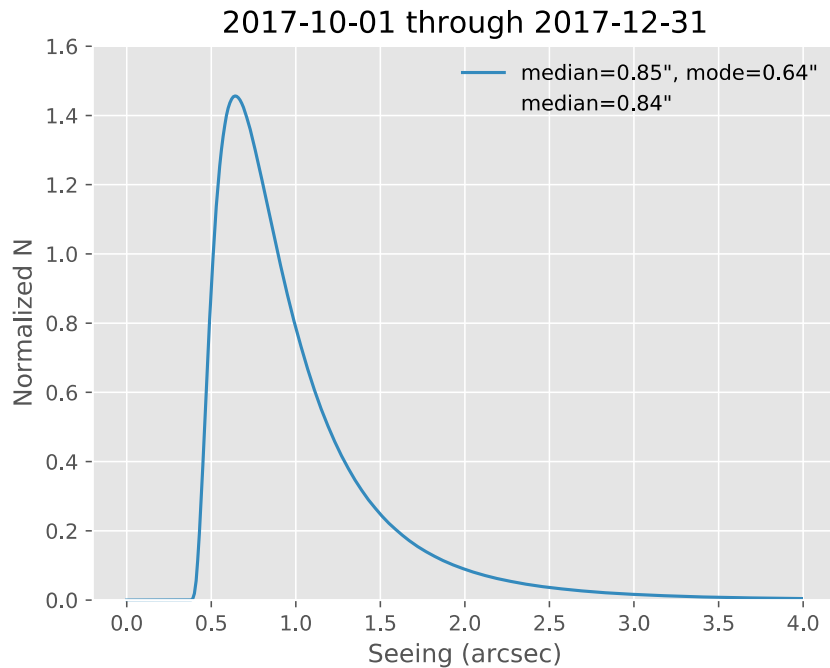


Figure 12. Histogram of seeing data for the 4th quarter of 2017.

The monthly trends were pretty stark overall as seen in Figure 13. October had very good conditions with a median of 0.71", and many instances of sub-0.5" seeing. November was somewhat worse with the numbers dominated by the week and a half of Binospec data, but was still sub-1.0" the majority of the time. December was quite bad overall, however, and was dominated by persistent easterly winds from very strong high pressure over the Great Plains. This is even more clearly shown in the nightly seeing statistics (Figure 14) where the seeing obviously blows up in mid-December, but settles back down by the end of the month.

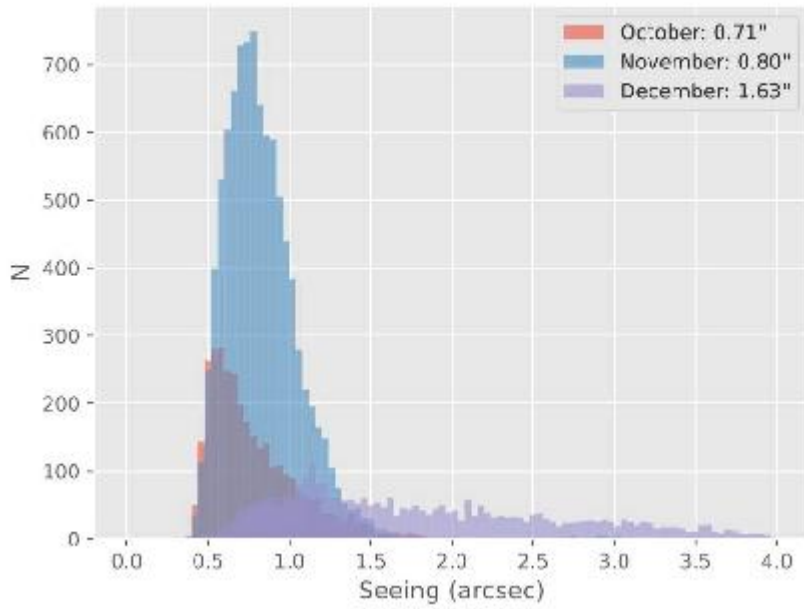


Figure 13. Monthly seeing histograms for the 4th quarter of 2017.

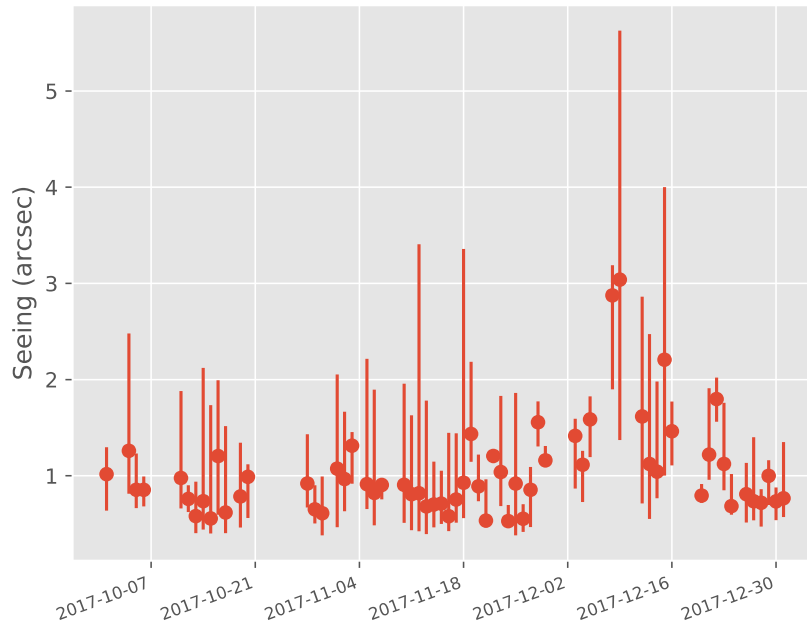


Figure 14. Median, minimum, and maximum seeing for each night of the 4th quarter of 2017.

Interestingly, the dichotomy between seeing measured in the first and second halves of the nights is not evident in this quarter as it had been previously (Figure 15). This time, the seeing is formally slightly worse in the second half, a reverse of the previous trend.

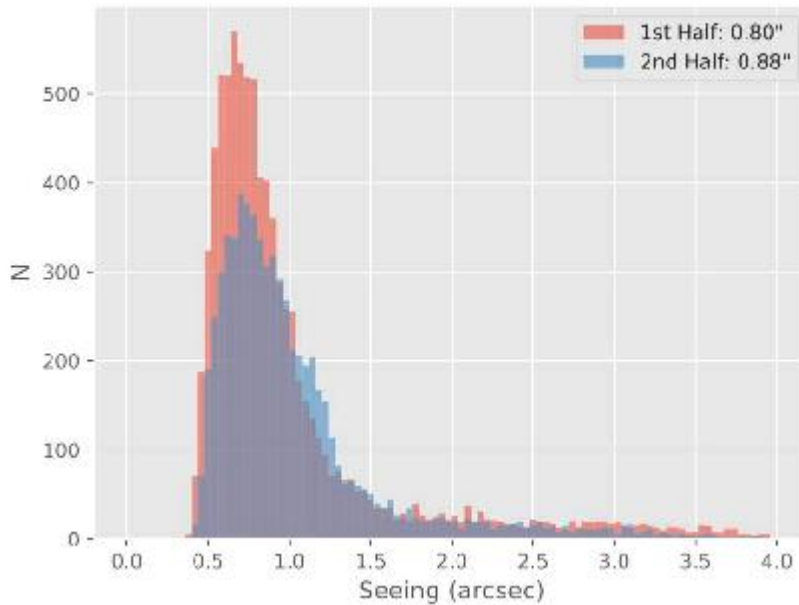


Figure 15. Histograms of seeing measured in the first and second halves of the night.

However, given the large amount of Binospec seeing measurements collected during bad weather and easterly winds in December, it's worth breaking this out per month.

As seen in Figure 16, it's actually November where the second half seeing is worse than the first half. For the other two months, the second half seeing is clearly better as we've seen in previous data. The difference in December is pretty stark, with a median of almost 2" in the first half and improving to 1.4" in the second half.

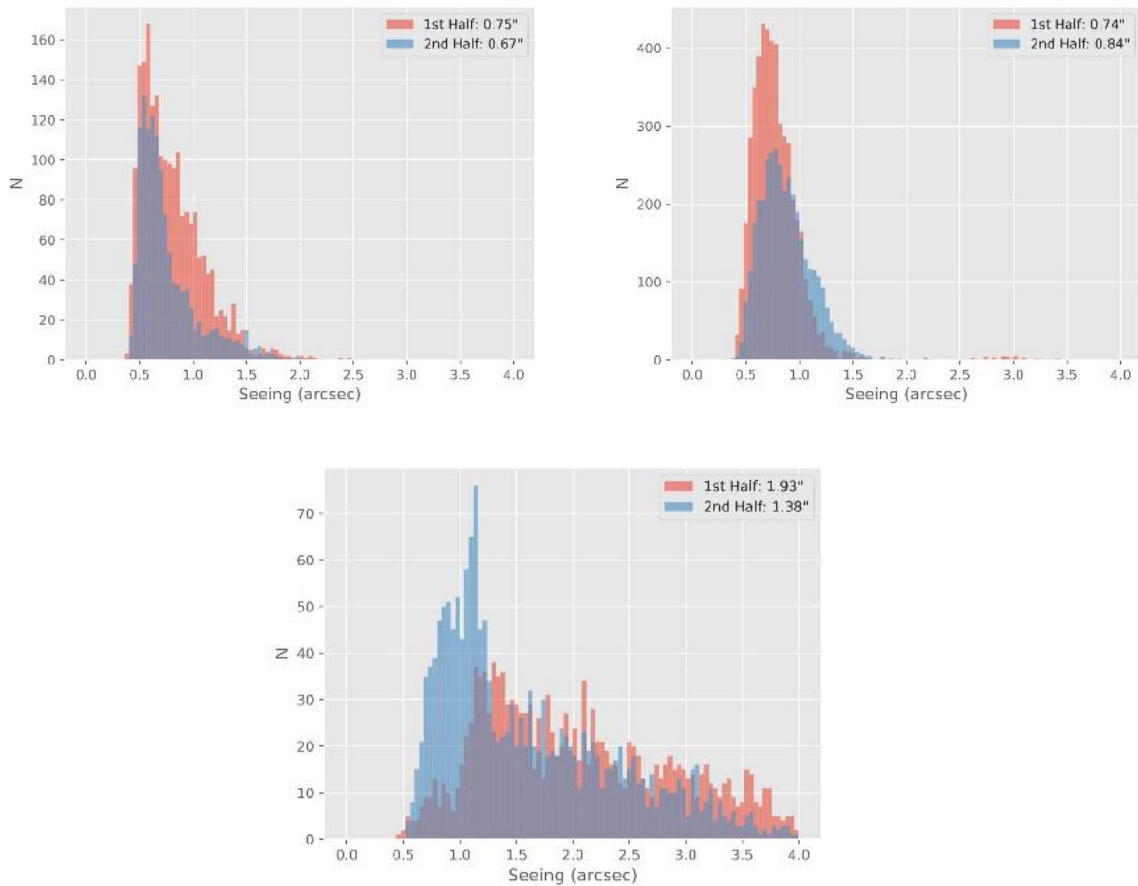


Figure 16. First/second half seeing histograms for October (left), November (right), and December (lower).

User Support

Web Pages

B. Weiner hosted and is continuing to update a web page with technical information for Binospec observers, used for preparation of 2018A shared-risk Binospec proposals. This has been updated substantially during and after commissioning, and will eventually be migrated to the MMT0 website. B. Weiner also wrote and is hosting a web page with a walkthrough/tutorial on the BinoMask slitmask design software, which will be used to aid users in mask and catalog preparation.

Remote Observing

The MMT0 supported 23 nights of remote observing this quarter. Seven and a half nights were for CfA observers, with fifteen and a half nights for UA observers. Remote observing has been a crucial

part of responding to instrument failures, allowing staff to schedule observers immediately with Blue or Red Channel, preventing the total loss of nights.

Data Quality Assessment

Data Archive

An interface/dialog has been added to the users' queue observing/catalog page so that users can download their Binospec data files from a completed observation. This addition was made by D. Porter with input from B. Weiner and S. Moran.

Reduction Procedures

Documentation

Document Database

Procedures

Public Relations and Outreach

Visitors and Tours

11/15/17 – T. Connor and D. Zellner, both of Steward Observatory, provided a tour of the MMTO for a TAO (Tokyo Atacama Observatory) guest. The TAO will also have a 6.5-m mirror and will be located in Chile.

11/18/17 – M. Alegria gave a tour of the MMTO to Dr. Vishnu Reddy (Asst. Professor, Planetary Sciences, UA) and members of the US Air Force.

Public Presentations

B. Weiner gave a public talk on November 17 at the Canoa Ranch star party (supported by Whipple Observatory and Pima County Parks) on dwarf galaxies surveyed with MMT/Hectospec.

G. Williams gave a talk at the Whipple Observatory Star Party on December 15.

J. Hinz organized and announced the speakers for the 2018 Smithsonian Lectures on Astronomy held in Green Valley every spring at the Recreation Center West. It will be the 48th year of the series.

MMTO in the Media

Site Protection

Appendix I - Publications

MMT Related Scientific Publications

(An online publication list can be found in the MMTO ADS library at <http://www.mmtto.org/node/244>)

- 17-56 Constraining the Milky Way Mass with Hypervelocity Stars
G. Fragione and A. Loeb
NewA, **55**, 32
- 17-57 Discovery of 16 New z 5.5 Quasars: Filling in the Redshift Gap of Quasar Color Selection
J. Yang, X. Fan, X.-B. Wu, et al.
AJ, **153**, 184
- 17-58 Light and Heavy Element Abundance Variations in the Outer Halo Globular Cluster NGC 6229
C.I. Johnson, N. Caldwell, R.M. Rich, et al.
AJ, **154**, 155
- 17-59 Clustering on Very Small Scales from a Large Sample of Confirmed Quasar Pairs: Does Quasar Clustering Track from Mpc to kpc scales?
S. Eftekharzadeh, A.D. Myers, J.F. Hennawi, et al.
MNRAS, **468**, 77
- 17-60 Trace Hydrogen in Helium Atmosphere White Dwarfs as a Possible Signature of Water Accretion
F. Gentile, P. Nicola, B.T. Gänsicke, J. Farihi, et al.
MNRAS, **468**, 971
- 17-61 Time-resolved Spectropolarimetric Observations of Polars WX LMi and BY Cam
D.T. Ozdarcı, P.S. Smith, and V. Keskin
MNRAS, **468**, 2923
- 17-62 Investigating the Unification of LOFAR-detected Powerful AGN in the Boötes Field
L.K. Morabito, W.L. Williams, K.J. Duncan, et al.
MNRAS, **469**, 1883
- 17-63 The First Baade-Wesselink Analysis of Blazhko RR Lyrae Stars: Discrepancies Between Photometrically and Spectroscopically Determined Radius Variations
J. Jurcsik and G. Hajdu
MNRAS, **470**, 617
- 17-64 The Fine Line Between Normal and Starburst Galaxies
N. Lee, K. Sheth, K.S. Scott, et al.
MNRAS, **471**, 2124

- 17-65 The Statistical Properties of Neutral Gas at $z < 1.65$ from UV Measurements of Damped Lyman Alpha Systems
S.M. Rao, D.A. Turnshek, G.M. Sardane, E.M. Monier
MNRAS, **471**, 3428
- 17-66 A Gemini Snapshot Survey for Double Degenerates
M. Kilic, W.R. Brown, A. Gianninas, et al.
MNRAS, **471**, 4218
- 17-67 The Nearby Type Ibn Supernova 2015G: Signatures of Asymmetry and Progenitor Constraints
I. Shivvers, WK Zheng, S.D. Van Dyk, et al.
MNRAS, **471**, 4381
- 17-68 Ultraviolet Spectra of Extreme Nearby Star-forming Regions – Approaching a Local Reference Sample for JWST
P. Senchyna, D.P. Stark, A. Vidal-Garcia, et al.
MNRAS, **472**, 2608
- 17-69 Galaxy Cluster Luminosities and Colours, and their Dependence on Cluster Mass and Merger State
S.L. Mulroy, S.L. McGee, S. Gillman, et al.
MNRAS, **472**, 3246
- 17-70 First Discoveries of $z > 6$ Quasars with the DECam Legacy Survey and UKIRT Hemisphere Survey
F. Wang, X. Fan, J. Yang, et al.
ApJ, **839**, 27
- 17-71 Cosmic Reionization on Computers: Properties of the Post-reionization IGM
N.Y. Gnedin, G.D. Becker, X. Fan
ApJ, **841**, 26
- 17-72 A Tale of Two Imposters: SN2002kg and SN1954J in NGC 2403
R.M. Humphreys, K. Davidson, S.D. Van Dyk, et al.
ApJ, **848**, 86
- 17-73 Galaxy Evolution in Merging Clusters: The Passive Core of the “Train Wreck” Cluster of Galaxies, A 520
B. Deshev, A. Finoguenov, M. Verdugo, et al.
A&A, **607**, 131
- 17-74 Physical Properties of 15 Quasars at $z \gtrsim 6.5$
C. Mazzucchelli, E. Bañados, B.P. Venemans, et al.
ApJ, **849**, 91

- 17-75 A Spectroscopic Survey of the Fields of 28 Strong Gravitational Lenses: Implications for H_0
M.L. Wilson, A.I. Zabludoff, C.R. Keeton, et al.
ApJ, **850**, 94
- 17-76 Type II Supernova Light Curves and Spectra from the CfA
M. Hicken, A.S. Friedman, S. Blondin, et al.
ApJS, **233**, 6
- 17-77 Ionized-gas Kinematics Along the Large-scale Radio Jets in Type-2 AGNs
H.A.N. Le, J.-H. Woo, D. Son, et al.
ApJ, **851**, 8
- 17-78 Optical Design of Infrared Pyramid Wavefront Sensor for the MMT
S. Chen, S. Sivanandam, S. Liu, et al.
Proc. SPIE, **10401**, 104011H
- 17-79 Mass-Metallicity Relation of Dwarf Galaxies and its Dependency on Time: Clues from Resolved Systems and Comparisons with Massive Galaxies
S.L. Hidalgo
A&A, **606**, 115
- 17-80 Blazar Spectral Variability as Explained by a Twisted Inhomogeneous Jet
C.M. Raiteri, M. Villata, J.A. Acosta-Pulido, et al.
Nature Lett., **552**, 374

MMT Technical Memoranda / Reports

Non-MMT Related Staff Publications

Appendix II - Service Request (SR) and Response Summary: October - December, 2017

The MMT Service Request (SR) system is an online tool to track ongoing issues that arise primarily during telescope operations, although the system can be used throughout the day and night by the entire staff. Once an SR has been created, staff members create responses to address and eventually close the SR. These SRs and associated responses are logged into a relational database for later reference.

Figure 17 presents the distribution of SR responses by priority during the period of October through December 2017. As seen in the figure, most (54%) of the SRs are of Important Priority, 22% are Near-Critical Priority, 14% are Low Priority, 5% are Critical, and 5% Information Only each.

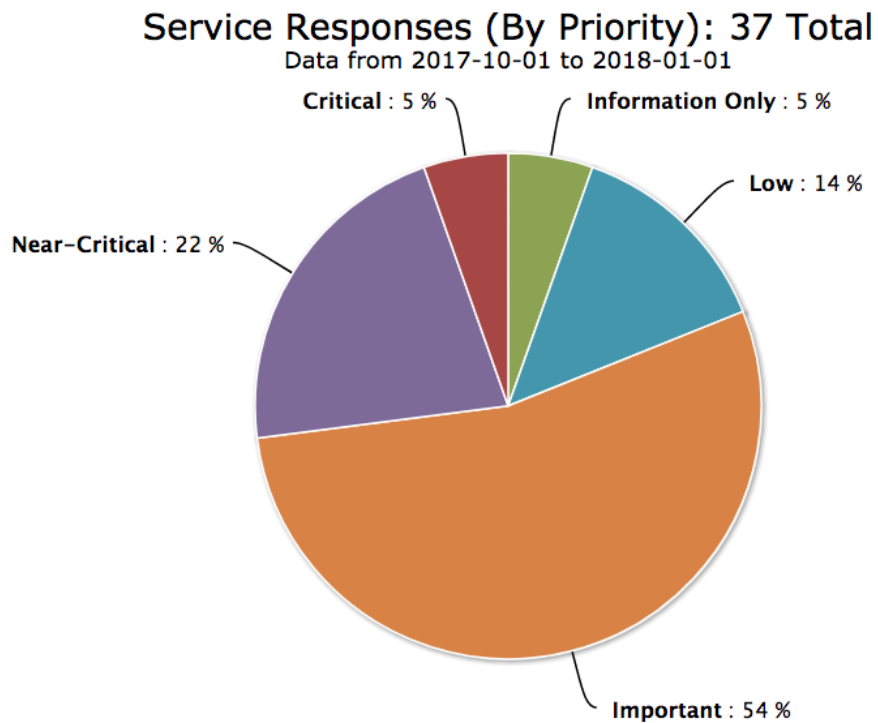


Figure 17. Service Request (SR) responses by priority during October through December 2017. 54% of the SRs were “Important,” while 22% were “Near-Critical” priority. 14% were Low priority, while Critical and Information-Only were 5% each.

“Critical” SRs address issues that are preventing telescope operation, while “Near-Critical” SRs relate to concerns that pose an imminent threat to continued telescope operation. There were a total of 37 SRs during this three-month period, compared with 41 for the previous reporting period. This number is less than normal for the SR system.

Figure 18 presents the same 37 SR responses grouped by category. These categories are further divided into subcategories for more detailed tracking of issues. Ten responses from October through

December are related to the “Telescope” category. These Telescope-related responses included many of the Critical and Near-Critical SRs. Nine responses were made under the “Cell” category while six responses were within the “Weather Systems” category. Responses also occurred in the “Building,” “Computers/Network,” “F9 Topbox,” “Instruments,” “Pit,” “Support Building,” and “Thermal System” categories.

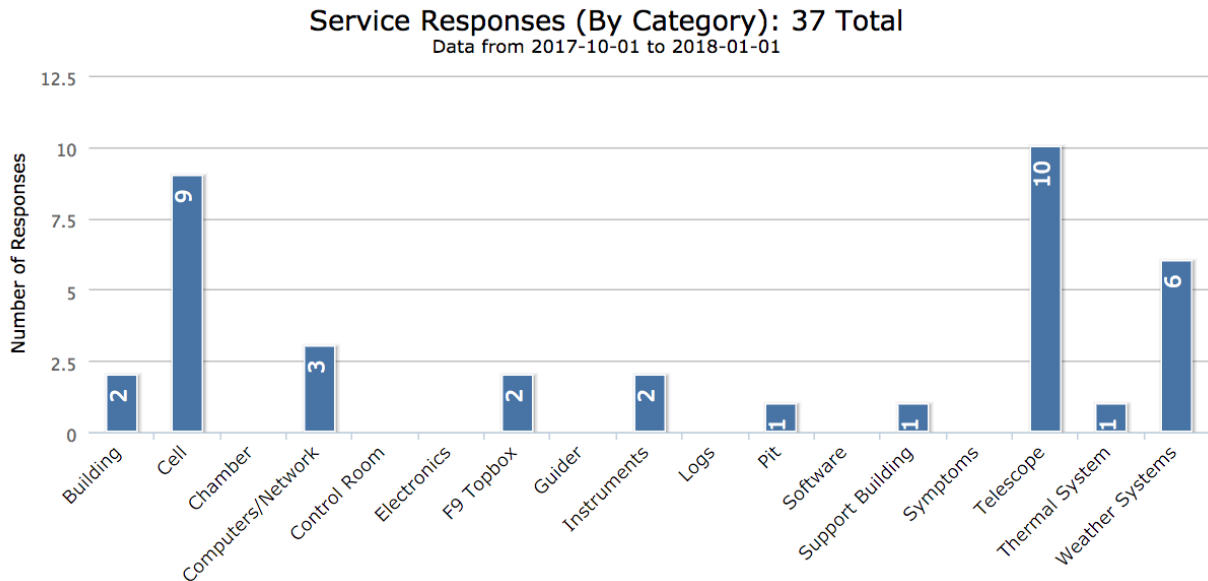


Figure 18. Service Request responses by category during October through December 2017. The majority of responses were within the “Telescope,” “Cell,” and “Weather Systems” categories. The number of responses is listed with the category.

Appendix III - Observing Statistics

The MMTO maintains a database containing relevant information pertaining to the operation of the telescope, facility instruments, and the weather. Details are given in the June 1985 monthly summary. The data attached to the back of this report are taken from that database.

Use of MMT Scientific Observing Time

October 2017

<u>Instrument</u>	<u>Nights Scheduled</u>	<u>Hours Scheduled</u>	<u>Lost to Weather</u>	<u>*Lost to Instrument</u>	<u>**Lost to Telescope</u>	<u>***Lost to Gen'l Facility</u>	<u>****Lost to Environment</u>	<u>Total Lost</u>
MMT SG	12.00	131.00	6.75	1.33	0.16	0.00	0.00	8.24
PI Instr	18.00	194.80	45.11	10.75	0.00	0.00	0.00	55.86
Engr	1.00	10.60	0.00	0.00	0.00	0.00	0.00	0.00
Sec Change	0.00	0.00	0.00	0.00	0.00	0.00	0.00	0.00
Total	31.00	336.40	51.86	12.08	0.16	0.00	0.00	64.10

Time Summary

Percentage of time scheduled for observing	96.8	* <u>Breakdown of hours lost to instrument</u>
Percentage of time scheduled for engineering	3.2	10.00 Hecto robot positioner failure
Percentage of time scheduled for sec/instr change	0.0	0.33 Red Channel bright stripes at blue end of chip
Percentage of time lost to weather	15.4	1.00 Red Channel guider issues
Percentage of time lost to instrument	3.6	0.75 MMIRS guis froze
Percentage of time lost to telescope	0.0	** <u>Breakdown of hours lost to telescope</u>
Percentage of time lost to general facility	0.0	0.16 M1 panic
Percentage of time lost to environment (non-weather)	0.0	
Percentage of time lost	19.1	

November 2017

<u>Instrument</u>	<u>Nights Scheduled</u>	<u>Hours Scheduled</u>	<u>Lost to Weather</u>	<u>*Lost to Instrument</u>	<u>**Lost to Telescope</u>	<u>***Lost to Gen'l Facility</u>	<u>****Lost to Environment</u>	<u>Total Lost</u>
MMT SG	13.00	153.10	39.50	0.00	3.00	0.00	0.00	42.50
PI Instr	14.00	160.60	53.50	0.00	0.00	0.00	0.00	53.50
Engr	3.00	34.90	0.00	0.00	0.00	0.00	0.00	0.00
Sec Change	0.00	0.00	0.00	0.00	0.00	0.00	0.00	0.00
Total	30.00	348.60	93.00	0.00	3.00	0.00	0.00	96.00

Time Summary

Percentage of time scheduled for observing	90.0	** <u>Breakdown of hours lost to telescope</u>
Percentage of time scheduled for engineering	10.0	3.00 Elevation oscillation issues
Percentage of time scheduled for sec/instr change	0.0	
Percentage of time lost to weather	26.7	
Percentage of time lost to instrument	0.0	
Percentage of time lost to telescope	0.9	
Percentage of time lost to general facility	0.0	
Percentage of time lost to environment (non-weather)	0.0	
Percentage of time lost	27.5	

Year to Date November 2017

<u>Instrument</u>	<u>Nights Scheduled</u>	<u>Hours Scheduled</u>	<u>Lost to Weather</u>	<u>Lost to Instrument</u>	<u>Lost to Telescope</u>	<u>Lost to Gen'l Facility</u>	<u>Lost to Environment</u>	<u>Total Lost</u>
MMT SG	89.00	907.70	311.44	6.75	3.41	1.25	0.00	322.85
PI Instr	200.00	1941.80	717.13	37.62	23.70	15.08	0.00	793.53
Engr	17.00	174.00	27.20	0.00	0.00	0.00	0.00	27.20
Sec Change	0.00	0.00	0.00	0.00	0.00	0.00	0.00	0.00
Total	306.00	3023.50	1055.77	44.37	27.11	16.33	0.00	1143.58

Time Summary Exclusive of Shutdown

Percentage of time scheduled for observing	94.2
Percentage of time scheduled for engineering	5.8
Percentage of time scheduled for sec/instr change	0.0
Percentage of time lost to weather	34.9
Percentage of time lost to instrument	1.5
Percentage of time lost to telescope	0.9
Percentage of time lost to general facility	0.5
Percentage of time lost to environment (non-weather)	0.0
Percentage of time lost	37.8

December 2017

<u>Instrument</u>	<u>Nights Scheduled</u>	<u>Hours Scheduled</u>	<u>Lost to Weather</u>	<u>*Lost to Instrument</u>	<u>**Lost to Telescope</u>	<u>***Lost to Gen'l Facility</u>	<u>****Lost to Environment</u>	<u>Total Lost</u>
MMT SG	12.00	143.70	42.98	0.00	0.25	0.00	0.00	43.23
PI Instr	15.00	179.80	81.15	0.00	3.00	0.00	0.00	84.15
Engr	3.00	35.80	22.15	0.00	0.00	0.00	0.00	22.15
Sec Change	0.00	0.00	0.00	0.00	0.00	0.00	0.00	0.00
Total	30.00	359.30	146.28	0.00	3.25	0.00	0.00	149.53

Time Summary

Percentage of time scheduled for observing	90.0
Percentage of time scheduled for engineering	10.0
Percentage of time scheduled for secondary change	0.0
Percentage of time lost to weather	40.7
Percentage of time lost to instrument	0.0
Percentage of time lost to telescope	0.9
Percentage of time lost to general facility	0.0
Percentage of time lost to environment	0.0
Percentage of time lost	41.6

** Breakdown of hours lost to telescope

0.25	M1 panic while using questionable WFS images
2.75	Hexapod oscillation
0.25	M1 panic

Year to Date December 2017

<u>Instrument</u>	<u>Nights Scheduled</u>	<u>Hours Scheduled</u>	<u>Lost to Weather</u>	<u>Lost to Instrument</u>	<u>Lost to Telescope</u>	<u>Lost to Gen'l Facility</u>	<u>Lost to Environment</u>	<u>Total Lost</u>
MMT SG	101.00	1051.40	354.42	6.75	3.66	1.25	0.00	366.08
PI Instr	215.00	2121.60	798.28	37.62	26.70	15.08	0.00	877.68
Engr	20.00	209.80	49.35	0.00	0.00	0.00	0.00	49.35
Sec Change	0.00	0.00	0.00	0.00	0.00	0.00	0.00	0.00
Total	336.00	3382.80	1202.05	44.37	30.36	16.33	0.00	1293.11

Time Summary Exclusive of Shutdown

Percentage of time scheduled for observing	93.8
Percentage of time scheduled for engineering	6.2
Percentage of time scheduled for secondary change	0.0
Percentage of time lost to weather	35.5
Percentage of time lost to instrument	1.3
Percentage of time lost to telescope	0.9
Percentage of time lost to general facility	0.5
Percentage of time lost to environment	0.0
Percentage of time lost	38.2